JAIST Repository
https://dspace.jaist.ac.jp/

Title	The impacts of electronic state hybridization on the binding energy of single phosphorus donor electrons in extremely downscaled silicon nanostructures
Author(s)	Anh, Le The; Moraru, Daniel; Manoharan, Muruganathan; Tabe, Michiharu; Mizuta, Hiroshi
Citation	Journal of Applied Physics, 116(6): 063705-1-063705-9
Issue Date	2014-08-12
Type	Journal Article
Text version	publisher
URL	http://hdl.handle.net/10119/12323
Rights	Copyright 2014 American Institute of Physics. This article may be downloaded for personal use only. Any other use requires prior permission of the author and the American Institute of Physics. The following article appeared in Le The Anh, Daniel Moraru, Muruganathan Manoharan, Michiharu Tabe, and Hiroshi Mizuta, Journal of Applied Physics, 116(6), 063705 (2014) and may be found at http://dx.doi.org/10.1063/1.4893181
Description	

JAIST
JAPAN
ADVANCED INSTITUTE OF
SCIENCE AND TECHNOLOGY

Japan Advanced Institute of Science and Technology

The impacts of electronic state hybridization on the binding energy of single phosphorus donor electrons in extremely downscaled silicon nanostructures

Le The Anh,[1,a)] Daniel Moraru,[2] Muruganathan Manoharan,[1] Michiharu Tabe,[2] and Hiroshi Mizuta[1,3]

[1]*School of Materials Science, Japan Advanced Institute of Science and Technology, Asahidai 1-1, Nomishi, Ishikawa 923-1292, Japan*

[2]*Research Institute of Electronics, Shizuoka University, 3-5-1 Johoku, Naka-ku, Hamamatsu 432-8011, Japan*

[3]*Nano Research Group, Electronics and Computer Science, University of Southampton, Highfield, Southampton, Hampshire SO17 1BJ, United Kingdom*

(Received 28 May 2014; accepted 4 August 2014; published online 12 August 2014)

We present the density functional theory calculations of the binding energy of the Phosphorus (P) donor electrons in extremely downscaled single P-doped Silicon (Si) nanorods. In past studies, the binding energy of donor electrons was evaluated for the Si nanostructures as the difference between the ionization energy for the single P-doped Si nanostructures and the electron affinity for the un-doped Si nanostructures. This definition does not take into account the strong interaction of donor electron states and Si electron states explicitly at the conductive states and results in a monotonous increase in the binding energy by reducing the nanostructure's dimensions. In this paper, we introduce a new approach to evaluate the binding energy of donor electrons by combining the projected density of states (PDOS) analysis and three-dimensional analysis of associated electron wavefunctions. This enables us to clarify a gradual change of the spatial distribution of the 3D electron wavefunctions (3DWFs) from the donor electron ground state, which is fully localized around the P donor site to the first conductive state, which spreads over the outer Si nanorods contributing to current conduction. We found that the energy of the first conductive state is capped near the top of the atomistic effective potential at the donor site with respect to the surrounding Si atoms in nanorods smaller than about 27 a_0. This results in the binding energy of approximately 1.5 eV, which is virtually independent on the nanorod's dimensions. This fact signifies a good tolerance of the binding energy, which governs the operating temperature of the single dopant-based transistors in practice. We also conducted the computationally heavy transmission calculations of the single P-doped Si nanorods connected to the source and drain electrodes. The calculated transmission spectra are discussed in comparison with the atomistic effective potential distributions and the PDOS-3DWFs method. © *2014 AIP Publishing LLC*. [http://dx.doi.org/10.1063/1.4893181]

I. INTRODUCTION

One of the primary objectives of past research on doping in semiconductors was to find dopants with a low binding energy E_b, such that they act as shallow donors, which can easily be ionized in bulk semiconductors at room temperature. Recently, the discrete nature of dopant atoms has attracted an increasing interest along with downscaling the sizes of MOSFETs to nanometer dimensions.[1–3] Variations of the MOSFET electronic characteristics become pronounced when the degree of spatial dopant fluctuation becomes comparable with the device dimensions.[4–6] A number of theoretical and experimental studies so far discussed the impacts of random dopant fluctuations on the significant variations in the threshold voltage and drive current of MOSFETs.[7–9]

On the other hand, the technological progress offers the possibility of utilizing individual dopant atoms to realize novel functional devices at nanometer scale.[10–12] One of the basic operations of these nanometer-scale devices is based on single-electron tunneling mediated by a single dopant.[10,11] The binding energy of donor electrons should be much higher than the thermal energy to ensure the operation of the single dopant devices at room temperature.[11] Therefore, it is important to estimate accurately the binding energy of donor electrons not only for the single dopant devices in particular but also for the nanometer-scale devices in general. To date, the binding energy of dopant electrons was defined as the difference between the ionization energy calculated for the P-doped Si nanostructures and the electron affinity calculated for the un-doped Si nanostructures. This definition was often used in many calculations from the tight binding calculations to the full DFT real-space calculations.[14–21] The first conductive state was determined through the electron affinity of the un-doped Si nanostructures. This definition, however, fails to include the strong interaction of electrons at excited states and P ions, which can be described by the hybridization of the donor electron states and the Si electron states in extremely downscaled Si nanostructures.

This hybridization undoubtedly takes a predominant role in the electronic and transport properties of the nanometer-scale devices along with the quantum confinement[13,14] and

[a)]Electronic mail: letheanh@jaist.ac.jp.

 © 2014 AIP Publishing LLC

[This article is copyrighted as indicated in the article. Reuse of AIP content is subject to the terms at: http://scitation.aip.org/termsconditions. Downloaded to] IP: 150.65.166.110 On: Tue, 21 Oct 2014 01:57:17

dielectric confinement effects.[15] In this study, for the first time, we investigate the binding energy at nano-scale, which considers the hybridization of the P donor electron states and Si electron states explicitly. By performing the DFT total energy calculation, we calculate the binding energy of the P donor electrons in the single P-doped Si nanorods from the projected density of state (PDOS) and 3D wavefunctions (3D-WFs) analysis. Finally, we conducted the transport calculation of the single P-doped Si nanorod connected to the source and drain electrodes. The transmission spectra show a good consistency with our new method.

This paper is organized as follows. Section II focuses on the computational method. Section III is dedicated to our results and discussion in the following order: PDOS and 3D-WFs analysis for isolated single P-doped Si nanorods (Sec. III A), PDOS analysis and transmission calculation for single P-doped Si nanorods with two Au electrodes (Sec. III B). Finally, we summarize our results in section IV.

II. METHODOLOGY

We have used the isolated Si nanorods with the ⟨100⟩ growth orientation in our simulations. To calculate the transmission spectra, the Si nanorods are connected to two semi-infinite Au electrodes. In this section, we discuss the structures used in our simulation and the computational method.

A. Structures of our models

The Si nanorods used in this study are built with the ⟨100⟩ orientation along the Z direction. The Si nanorods are covered with H atoms in order to passivate all of the dangling bonds. To investigate the effect of the quantum confinement on the electronic properties of the nanorods, we built five Si nanorods—$Si_{12}H_{28}P$, $Si_{61}H_{75}P$, $Si_{167}H_{147}P$, $Si_{357}H_{243}P$, and $Si_{652}H_{364}P$ with different sizes. The shapes of the five nanorods are analogous. In all these structures, we consider the P atom at the center substitutional site. Table I shows the dimensions of five Si nanorods along the X, Y, and Z axes. We label five Si nanorods—$Si_{12}H_{28}P$, $Si_{61}H_{75}P$, $Si_{167}H_{147}P$, $Si_{357}H_{243}P$, and $Si_{652}H_{364}P$ as SNR-A, SNR-B, SNR-C, SNR-D, and SNR-E, respectively. The average radius R_{avg} $((R_x + R_y + R_z)/3)$ is also reported in Table I, a_0 $(=0.53\text{Å})$ is the Bohr radius for the Hydrogen model. Figure 1(a) shows the views of SNR-B ($Si_{61}H_{75}P$) on the XY and XZ planes. The five SNRs have been embedded in large supercells in order to prevent interactions between the periodic replicas (about 20Åof vacuum separates neighboring clusters in the X, Y, and Z directions). To build single P-doped Si nanorods with two electrodes, we used two semi-infinite Au nanowires as the left lead and right lead as shown in Fig. 1(b). The channels are SNRs. Due to the large scale calculation, the number of Au atoms in each lead is optimized to 20. The distance between the lead interfaces and the nanorods is about 1.5 Å. The Z ⟨100⟩ direction is set as the transport direction from the left lead to the right lead. To minimize the hybridization between the states from two electrodes and the states of the nanorods, fully hydrogen terminated Si nanorods were used.

TABLE I. The dimensions of five Si nanorods labeled from SNR-A to SNR-E in the order of increase of the size.

	R_x (a_0)	R_y (a_0)	R_z (a_0)	R_{avg} (a_0)
SNR-A (Si12H28P)	6.73	4.18	9.28	6.73
SNR-B (Si61H75P)	11.84	6.66	16.96	11.82
SNR-C (Si167H147P)	16.96	9.37	24.62	16.98
SNR-D (Si357H243P)	22.07	12.05	32.43	22.18
SNR-E (Si652H364P)	27.20	14.49	40.05	27.24

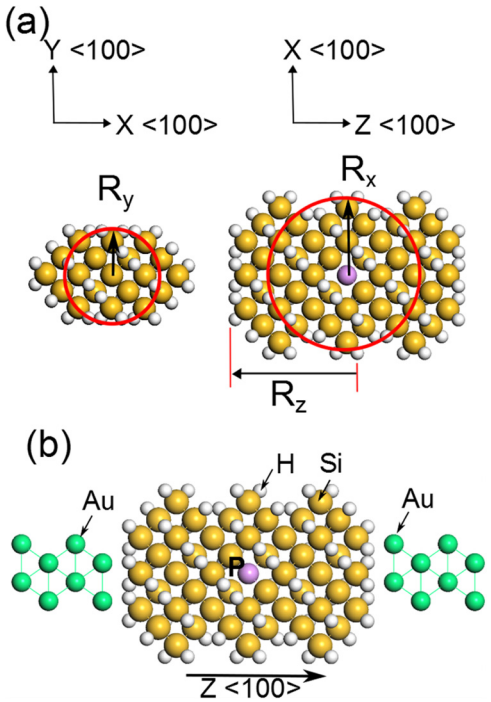

FIG. 1. (a) The single P-doped Si nanorod SNR-B ($Si_{61}H_{75}P$) viewed on the XY and XZ planes, (b) The view of SNR-B ($Si_{61}H_{75}P$) with two Au electrodes (named SNRD-B in Sec. III C) on the XZ plane. The white, yellow, green, and blue balls represent H, Si, Au, and P atoms, respectively.

B. Computational method

The first-principles calculations were performed using the code OpenMX,[22] which is based on density functional theories (DFT),[23] norm-conserving pseudopotentials,[24–28] and pseudoatomic localized basis functions.[29] All calculations are performed by using generalized gradient approximation (GGA) PBE version of the exchange-correlation potential.[30] The convergence threshold for the self-consistent field (SCF) iteration is 10^{-6} Hartree. The pseudo-atomic orbitals are used as basis functions to expand one-particle Kohn-Sham wave functions. The cut-off radius of the basis functions is 7.0 Å. Due to the large-scale calculation, only s-, p-, and d-state radical functions are used to represent the basis functions of Si, P, H, and Au. The k grid $1\times2\times3$ is used for the SCF calculation.

For the isolated Si nanorods, we use the conventional diagonalization method in the SCF iterations. For the Si nanorods sandwiched by two semi-infinite Au electrodes, we use the non-equilibrium Green's function (NEGF) method within the collinear DFT,[31] which is implemented in the

[This article is copyrighted as indicated in the article. Reuse of AIP content is subject to the terms at: http://scitation.aip.org/termsconditions. Downloaded to] IP: 150.65.166.110 On: Tue, 21 Oct 2014 01:57:17

OpenMX code in the SCF iteration. The NEGF method enables us to calculate the transmission spectra of electrons through the SNRs from the left to the right lead.

III. RESULTS AND DISCUSSION

A. The hybridization of the P electron states and Si electron states

It is well known that, in an un-doped Si nanostructure, the lowest unoccupied orbital is degenerated into three groups: one A_1 state, one threefold T_2 state, and one twofold E state.[13,20] The A_1 orbital has s-like symmetry on the center of nanostructure. The T_2 and E orbitals have a node on the center. The inter-valley couplings split these states. According to the tight binding calculation,[13] the splitings in spherical un-doped Si quantumdot range from 0.1 meV for diameter 10.32 nm up to 68 meV for diameter 1.85 nm. As for the P-doped Si nanostructures, we calculate the splitings of the A_1, T_2, and E states in SNR-B with average diameter of 1.25 nm. Figure 2 shows the projected density of states onto the P donor with Gaussian broadening of 0.15 eV and the Kohn-Sham energy levels from 0 eV up to 5 eV with respect to the Fermi level in the SNR-B ($Si_{61}H_{75}P$) with average diameter of 1.25 nm. The donor ground state is at 0 eV the LUMO state. The excited donor states LUMO + 1, LUMO + 2, and LUMO + 3 are shown in Fig. 2. We denote the LUMO + i is the ith excited state above the donor ground state LUMO. The A_1 state is the donor ground state. The T_2 state is the LUMO + 2. The E state is the LUMO + 10 state, which is not indicated in Fig. 2. Due to the Gaussian broadening in the PDOS spectrum, one PDOS peak may consist of numbers of quantum states. The splitings between the A_1-T_2 and T_2-E in SNR-B are 350 meV and 600 meV, which are much larger than the splitings in the tight binding calculation.[13] Such enhancement of the spliting is well known due to the strong quantum confinement of the central-cell donor potential in nano Si.[32] Next, we will study the hybridization of the P electron states and Si electron states in Si nanorods.

Figure 3 shows the top and side view of the wavefunctions of the A_1, T_2 and E states in the SNR-B on the XZ and YZ planes, respectively. As we can see that the A_1 orbital has a large projection on the center dopant atom compared to T_2 and E states. Therefore, the dopant in the center stabilizes the A_1 state more than the T_2 and E state. This leads to the fact that the donor ground state is the A_1 state. In Fig. 3, we show the s, p, and d components of the PDOS onto the P atom and onto the first neighboring Si atom in SNR-B. The A_1 state has a contribution not only from the s orbital of the P dopant but also from the p and d orbital of the first neighboring Si. The T_2 state has contributions from the p and d orbital of the P dopant and the s, p, and d orbitals of the first neighboring Si. The E state has contributions from the s, p, and d orbital of the P dopant and the s, p, and d orbital of the first neighboring Si. This means there is hybridization between the P electron states and Si electron states in SNRs. The hybridization can be observed not only at the donor ground state A_1 but also at the donor excited states such as T_2 and E.

In bulk Si, the first conductive state is considered as the lowest unoccupied state of the un-doped Si crystals. In nanostructures, there is hybridization between the P electron states and Si electron states at donor ground state and donor excited states as well. The hybridization becomes significantly strong when the sizes of Si nanostructures are smaller than the Bohr radius of P donor in bulk Si ($\sim 40\ a_0$) because the electrons are confined by the size of the nanostructures and continue to interact with the P donor at the higher-energy excited states. This leads to the fact that the hybridization must be taken into account to determine the first conductive states in Si nanostructures. The next section will

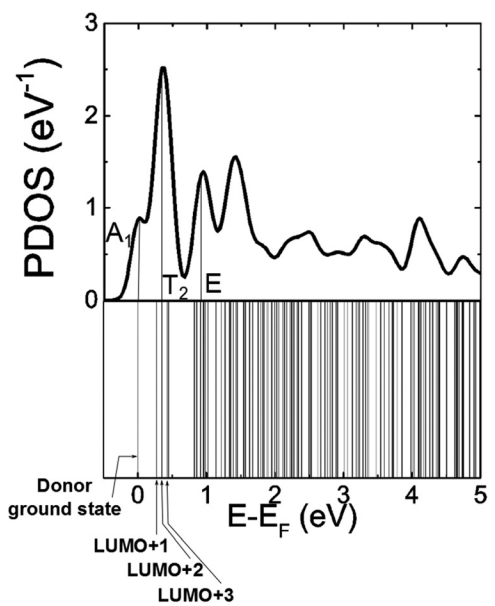

FIG. 2. Upper: The projected density of states onto the P atom in SNR-B. Lower: the Kohn-Sham energy levels with respect to the Fermi energy, the position of the A_1, T_2, and E states are indicated.

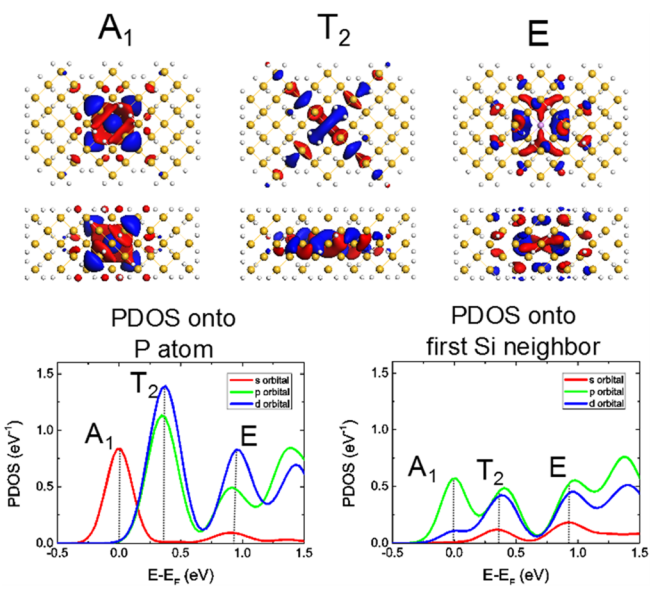

FIG. 3. Upper: The top and side views of the wavefunctions of the A_1, T_2 and E states in SNR-B on the XZ and YZ planes, respectively; Lower: The s, p, and d components of the PDOS onto the P atom and onto the first neighboring Si atom.

[This article is copyrighted as indicated in the article. Reuse of AIP content is subject to the terms at: http://scitation.aip.org/termsconditions. Downloaded to] IP: 150.65.166.110 On: Tue, 21 Oct 2014 01:57:17

discuss how to find the first conductive states in SNRs and the binding energy of the donor electrons.

B. The first conductive state and binding energy calculation for isolated Si nanorods

As we discussed in the previous section, the P electron states hybridize with the Si electron states. The weight of the contribution of the P electron states is important to determine how strongly the donor electrons interact with the P dopant in the nanostructures. Based on the change of the weight of the contribution of the P electron states, we can find the first conductive state relatively to the donor ground state. Let us consider which states in the density of states belong to which atoms in a nanostructure. This can be qualitatively considered by using the PDOS, which is obtained by projecting the wavefunction onto localized atomic orbitals. Therefore, the total DOS can be resolved into partial components PDOS onto an individual atom. The ratio PDOS/DOS, where PDOS is the projected density of states onto the P donor, DOS is the total density of states, presents the relative weight of the states associated to the P dopant against the states of the whole system. This ratio can be attributed to the contribution of the P electron states to the states of the whole system. Figure 4 shows the PDOS onto the P atoms and the ratios PDOS/DOS of SNR-A, SNR-B, SNR-C, SNR-D, and SNR-E. The five Si nanorods were embedded in large vacuum supercells in order to prevent interactions between the periodic replicas (about 20Åof vacuum separates neighboring nanorods in the X, Y, and Z directions). The Fermi level is set at 0 eV. The A_1 donor ground states are at 0 eV—the Fermi level. We can see from Fig. 4 that the ratios PDOS/DOS at low energy regime (below the dashed blue lines) are high and then decrease as energy increases. This can be interpreted as follows: At low energy levels near the donor ground state, the relative weight of the P electron states is high due to the strong confinement from the atomistic donor potential. At higher energy levels (above the dashed blue line), the relative weight is low due to the decreasing confinement. As a result, the ratios PDOS/DOS decrease relatively close to zero. Therefore, based on the change of the ratios PDOS/DOS, we can estimate directly the binding energy of the donor electrons in SNRs. We consider the position of the first conductive state is at the energy, where the ratio PDOS/DOS starts to become close to zero. For the SNR-A, SNR-B, SNR-C, SNR-D, and SNR-E, the first conductive states are estimated as the positions of the dashed blue lines.

To clarify the exact positions of the first conductive states in SNRs, we analyze the 3D wavefunctions associated to the donor ground states and the donor excited states. Figure 5(a) shows the projections of the wavefunction squares along the [100] direction associated to the donor ground state and seven donor excited states: LUMO + 3, LUMO + 9, LUMO + 24, LUMO + 28, LUMO + 32, LUMO + 74, and LUMO + 125 of the nanorod SNR-B ($Si_{61}H_{75}P$). For the convenient presentation, we only show seven donor excited states. Z is the coordinate along the [100] direction. The P atom is at the center, which is 15 Å

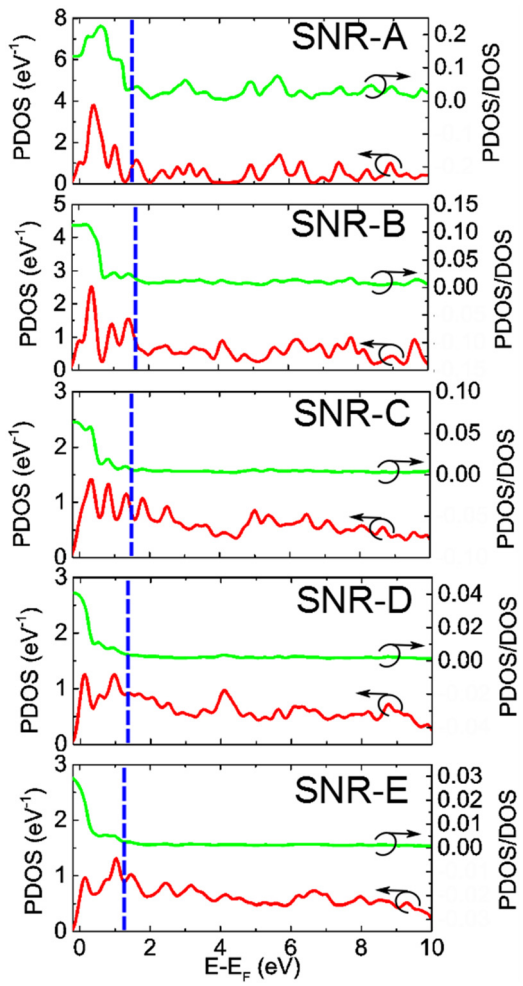

FIG. 4. The PDOS (red) onto the P atom and the ratio PDOS/DOS (green) of the nanorods SNR-A, SNR-B, SNR-C, SNR-D, and SNR-E. The dashed blue lines present the positions of the first conductive states.

away from the origin. We can see from Fig. 5(a) that the projections of the wavefunction squares near the center P atom gradually decrease from donor ground state LUMO to the LUMO + 28. But from the LUMO + 28, the decrease cannot be observed clearly. This is consistent with the PDOS analysis that the ratio PDOS/DOS rapidly changes at low energy regime and then become relatively close to zero at the critical energies. The energy level of the LUMO + 28 is 1.62 eV, is which equal to the critical energy (the position of the dashed blue line) found by the PDOS analysis. The right panels in Fig. 5(a) shows the wavefunction visualization of the state LUMO + 28 viewed on the XZ (upper panel) and YZ (lower panel) planes. We can see that the wavefunction of the state LUMO + 28 spreads throughout the structure without any significant localization. This suggests that electrons can successfully transport throughout the structures at this state. By combining the PDOS and the 3D-wavefunction analyses, we find that the energy level of the first conductive state in SNR-B ($Si_{61}H_{75}P$) is 1.62 eV. Similarly, the energy levels of the first conductive states in SNR-A, SNR-C, SNR-D, and SNR-E are 1.36 eV, 1.42 eV, 1.36 eV, and 1.21 eV, respectively. The binding energy is calculated as a difference between the A_1 donor ground state and the first conductive

[This article is copyrighted as indicated in the article. Reuse of AIP content is subject to the terms at: http://scitation.aip.org/termsconditions. Downloaded to] IP: 150.65.166.110 On: Tue, 21 Oct 2014 01:57:17

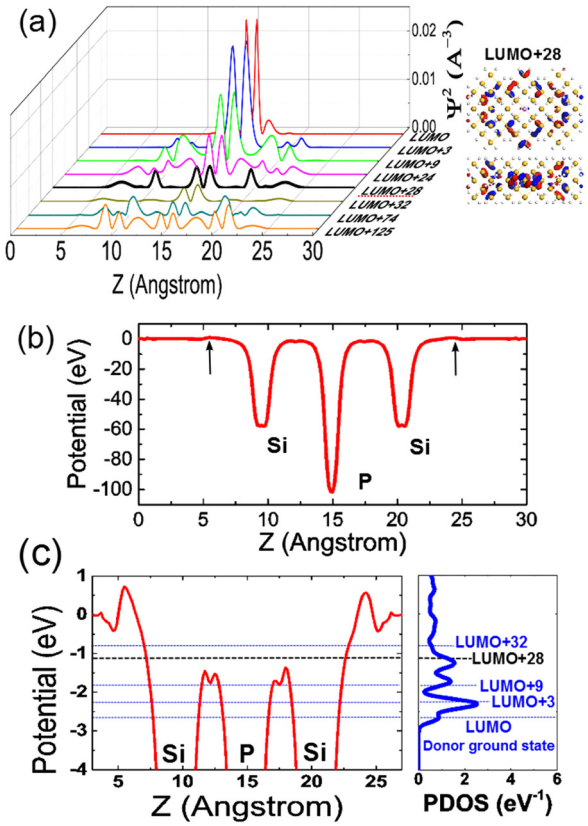

FIG. 5. (a) The projections of wavefunction squares of the A1 donor ground state (LUMO) and donor excited states in SNR-B along Z [100] direction, the right panel shows the wavefunction visualization of the donor excited state LUMO + 28 viewed on the XZ (upper panel) and YZ (lower panel) planes; (b) The atomistic effective potential of SNR-B along the Z direction, the arrows indicate the edge of the nanorod; (c) The atomistic effective potential of SNR-B along the Z direction plotted with the electronic energy levels, the lines show the positions of the LUMO- donor ground state and the donor excited states.

state. The A_1 donor ground states were found at the Fermi level 0 eV for five SNRs. Hence, the binding energies equal to the energy level of the first conductive states in five SNRs.

As we can see from Fig. 4 that the positions of the first conductive states (the positions of the dashed blue lines) do not monotonously increase toward higher energies when the size of the nanorods decrease according to the simple quantum confinement effect. In order to understand the mechanism behind this trend, we investigate the atomistic effective potential in SNRs. The atomistic effective potential is defined as the sum of the neutral atom potential and the Hartree potential, which considers the Coulomb electron-electron interactions.[33,34] We plot in Fig. 5(b), the atomistic effective potential of SNR-B. The two arrows indicate the edge of the nanorod. The atomistic effective potential at the P donor site is deeper than that at the Si sites. This causes the strong localization of wavefunction of electrons near the P atom site at donor ground state, which is shown with large projections of the wavefunction squares of the state LUMO near the center P atom in Fig. 5(a). Figure 5(c) shows the energy levels of donor ground state and donor excited states with the atomistic effective potential. We can see that the state LUMO + 28 is near above the top of the atomistic effective potential at the P atom. Above the top, the interaction between the donor electrons and the core P ion is small because the electrons are no longer confined by the atomistic effective potential at the P site. As a result, the projections of the wavefunction squares near the P atom keep small from the state LUMO + 28 to the higher-energy excited states as we can see from Fig. 5(a).

Figure 6 shows the atomistic effective potential of the SNR-A, SNR-B, SNR-C, SNR-D, and SNR-E. The left panels show the PDOS onto the P atoms. The positions of the first conductive states with respect to the vacuum level are denoted by the horizontal lines. When the sizes of the nanorods decrease from SNR-E to SNR-A, the first conductive state slightly lifts up due to the simple quantum confinement effect. But the interesting thing is that in addition to the simple quantum confinement effect, the atomistic effective potential distribution, which can be reflected into the hybridization of the P electron states and Si electron states, plays a role in determining the energy of the first conductive states. As we can see in Fig. 6, the positions of the first conductive states obtained from the PDOS-3DWFs method are still near the top of the atomistic effective potential at the P donor site. Except SNR-A with the average radius of 6.73 a_0, which close to the limit size of a P atom while retaining its sp^3 hybridization, the electrons are still confined by the extremely small size of the nanorod and continue to strongly interact with the P atom at high-energy states even above the top of the atomistic effective potential at the P site. Therefore, the

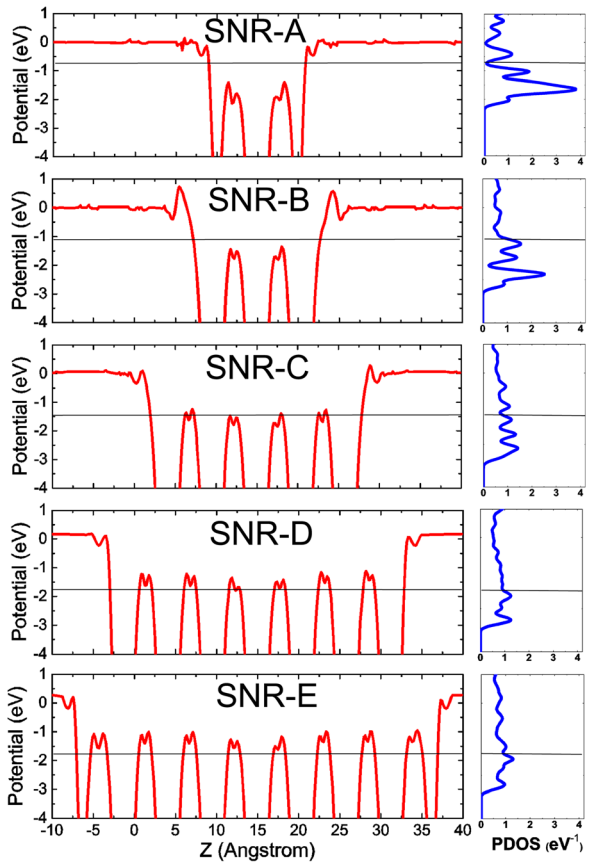

FIG. 6. The atomistic effective potential of the SNR-A, SNR-B, SNR-C, SNR-D, and SNR-E. The right side shows the PDOS onto the P atoms. The energy of the first conductive states with respect to the vacuum level is presented by the horizontal lines.

[This article is copyrighted as indicated in the article. Reuse of AIP content is subject to the terms at: http://scitation.aip.org/termsconditions. Downloaded to] IP: 150.65.166.110 On: Tue, 21 Oct 2014 01:57:17

first conductive state for SNR-A is a little bit far away from the top of the atomistic effective potentials. For other bigger structures, the electrons can be conductive near the top of the atomistic effective potentials due to weaker confinement. When the size decreases from bulk size to the size of SNR-E ($R_{avg} = 27.24\ a_0$), the first conductive state lifts up due to the increase of the quantum confinement and reaches near the top of the atomistic effective potential at the size of SNR-E. Above the top, the interaction between the donor electrons and the core P ion becomes small. The electron wavefunctions are more delocalized and can attribute to the conduction. If the size continues to decrease, the first conductive states still keep close to the tops of the atomistic effective potentials. As a result, the positions of the first conductive states weakly depend on the sizes when the structures are smaller than SNR-E.

According to previous published studies,[5,9,14] the binding energies of the P donor electrons in Si nanostructures are proportional to the inversed radii of the nanostructures due to the quantum confinement effect. In order to have direct comparison, we calculated the binding energies for the Si nanorods by using the conventional formula:[14]

$$E_b^{conv} = I_d - A_u,$$

where $I_d = E_d(n-1) - E_d(n)$ and $A_u = E_u(n) - E_u(n+1)$ are the ionization energy and electron affinity of the doped and un-doped systems, respectively. E_d and E_u are the total energy of the doped and un-doped systems.

In this conventional method, the first conductive state is determined as the lowest unoccupied state of the un-doped Si nanostructure. Hence, it fails to include the hybridization of the P electron states and Si electron states at the first conductive states. The binding energy obtained by this method is simply a decreasing function of the size due to the simple quantum confinement effect. Figure 7 shows the binding energy of the dopant electrons as a function of the nanorod's average radius, which is calculated by using the PDOS-3DWFs method and the conventional method. We can see in Fig. 7 that the conventional method shows the non-linear decrease of the binding energy when the size increases. While the PDOS-3DWFs method results in the binding energy of approximately 1.5 eV, which is virtually independent on the nanorod's dimensions.

In extremely small nanostructures, which are smaller than about 27 a_0, the energy of the first conductive states are capped near the tops of the atomistic effective potential at the P donor site, even for the smallest nanorod SNR-A. As a result, the binding energy calculated by the PDOS-3DWFs method shows the virtual independence of the size as can be seen from Fig. 7. This fact signifies a good tolerance of the binding energy, which governs the operating temperature of the single dopant-based transistors.[11]

C. The first conductive state and binding energy calculation for Si nanorods sandwiched with two Au electrodes

In this section, we study the single P-doped Si nanorods sandwiched with two semi-infinite Au electrodes as indicated in Fig. 1(b) in order to discuss the donor electron binding energy in terms of the transmission spectra.

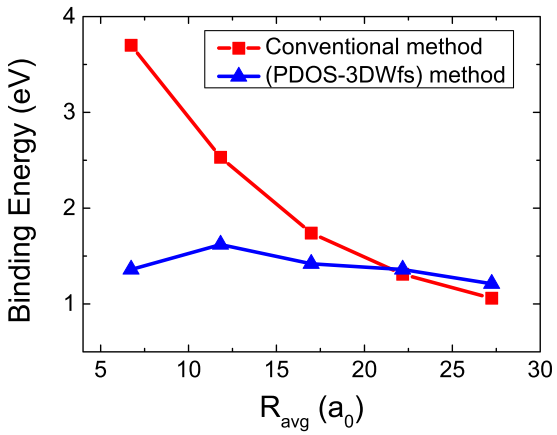

FIG. 7. The binding energy of the donor electrons as a function of the nanorod's average radius calculated by using the PDOS-3DWFs method and the conventional method. The lines are only for eye guide.

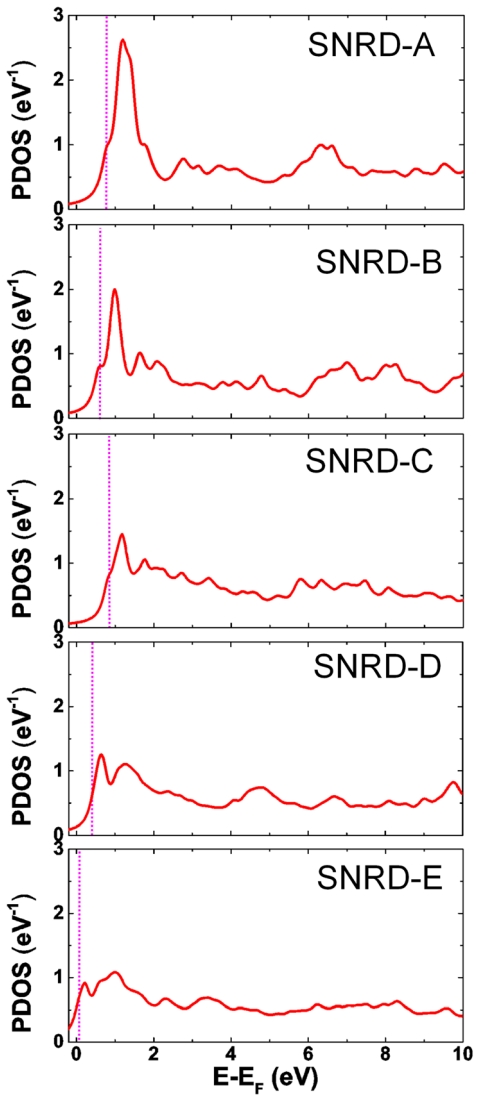

FIG. 8. The PDOS onto the P atom of five Si nanorods sandwiched with two electrodes SNRD-A to SNRD-E. The dashed purple lines present the positions of the donor ground states.

[This article is copyrighted as indicated in the article. Reuse of AIP content is subject to the terms at: http://scitation.aip.org/termsconditions. Downloaded to] IP: 150.65.166.110 On: Tue, 21 Oct 2014 01:57:17

We label the Si nanorods with electrodes Au-$Si_{12}H_{28}$P-Au, Au-$Si_{61}H_{75}$P-Au, Au-$Si_{167}H_{147}$P-Au, Au-$Si_{357}H_{243}$P-Au, and Au-$Si_{652}H_{364}$P-Au as SNRD-A, SNRD-B, SNRD-C, SNRD-D, and SNRD-E, respectively. Figure 8 shows the PDOS onto the P atoms of SNRD-A to SNRD-E. The energy of the donor ground states is marked by the dashed purple lines. In those calculations without any bias between the left and the right leads, the Fermi level of the left and the right leads were set at 0 eV, the donor ground states are then shifted to above the Fermi energy. Compared with the PDOS spectra for SNRs in Fig. 4, the individual peaks in the PDOS spectra obtained for SNRDs are more broadened. This is presumably caused by the imaginary part of the self-energies of the electrodes that is the broadening of quantum energy levels of SNRs induced by the electrodes. Moreover, the amplitudes of the PDOS at low energy regimes near the donor ground states gradually decrease from SNRD-A to SNRD-E. This reflects gradual delocalization of the wavefunction of the donor electrons. Therefore the evolutions of the PDOS with respect to energy can be used to estimate the binding energy of electrons as we discussed in Sec. II.

To prove the validity of the PDOS-3DWFs method in Sec. II, we carry out the transport calculations for the electrons through the Si nanorods with two electrodes. The transmission rate T(E) is calculated according to the Landauer formula, which is implemented in the OpenMX code.[21] Figure 9 shows the transmission spectra (blue) and the corresponding atomistic effective potentials (red) for five SNRDs. In those plots, the vacuum level was set to be 0 eV. The positions of the P, Si, and Au atoms along the Z direction are also indicated. The energy of the donor ground state D^0 is indicated by the lower horizontal black lines. We can see

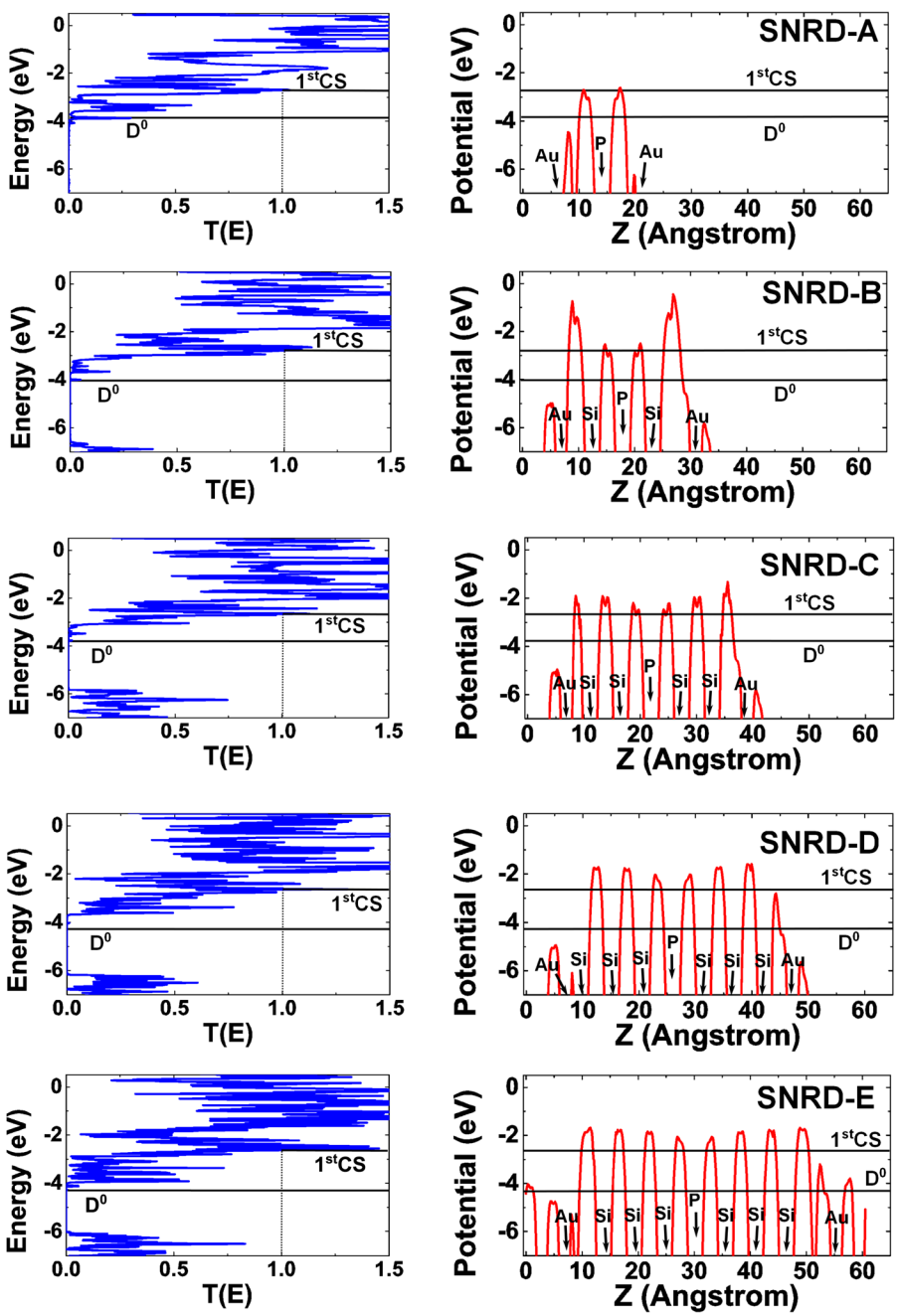

FIG. 9. Left panels: the transmission rates T(E); right panels: the corresponding atomistic effective potentials of the SNRD-A to SNRD-E. Two black lines show the positions of the donor ground states D^0 (the lower lines) and the first conductive states 1st CS (the upper lines).

[This article is copyrighted as indicated in the article. Reuse of AIP content is subject to the terms at: http://scitation.aip.org/termsconditions. Downloaded to] IP: 150.65.166.110 On: Tue, 21 Oct 2014 01:57:17

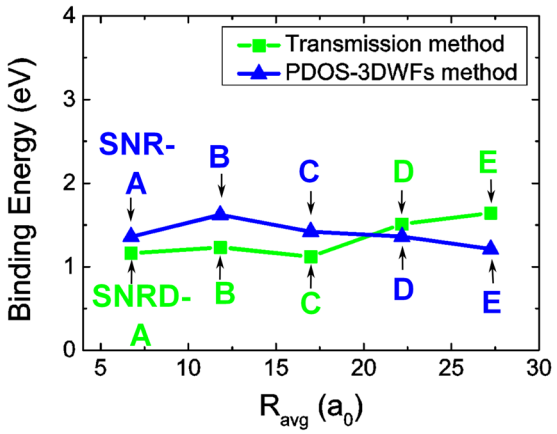

FIG. 10. The binding energies of the donor electrons as a function of the nanorod's average radius. The green squares and blue triangles represent the binding energies for SNRDs and SNRs calculated by the transmission method and the PDOS-3DWFs method, respectively. The lines are only for eye guide.

from Fig. 9 that the transmission rates are very low at the energy of the donor ground states and increase steeply with increasing energy. This is due to the strong contributions of the P electron states near the donor ground states, which cause the strong confinements of electrons at the P donor sites. The low transmission peaks near the donor ground states D^0 can reflect to the transports of single-electron tunneling mediated by single dopant.[12] The transmission rates increase as energy increases because the contributions from the P electron states gradually decrease and lead to the more delocalization of wavefunction of the donor electrons. To find the positions of the first conductive states, we define the positions where the transmission rates exceed one (100%) as the first conductive states. The positions of the first conductive states (1st CS) of SNRDs are indicated by the upper horizontal lines in Fig. 9. We can see from the corresponding atomistic effective potentials that the first conductive states energies are capped near the tops of the atomistic effective potentials at the P donor sites even for the smallest structure SNRD-A.

In Fig. 10, we compare the binding energies of five devices SNRD-A to SNRD-E calculated from the transmission spectra with those of five isolated Si nanorods SNR-A to SNR-E calculated from the PDOS-3DWFs method. The green squares represent the binding energies for SNRDs, while the blue triangles indicate the binding energy for SNRs. The virtually R_{avg} independence binding energy can be seen clearly for both methods. The binding energies are found around 1.5 eV. This is attributed to the capping of the first conductive states near the tops of the atomistic effective potentials at the P donor site.

IV. CONCLUSION

We have studied the electronic properties of the single P-doped Si nanorods by using the DFT calculation. It has been found that the hybridization of the P electron states and the Si electron states is significant not only at the donor ground state but also at the donor excited states in Si nanorods. The PDOS-3DWFs analysis enables us to clarify the gradually decreasing contribution of the P electron states from the donor ground states to the higher-energy donor excited states. Therefore, we can identify the first conductive states by using the PDOS-3DWFs analysis. We have calculated the binding energy of the donor electrons in the single P-doped Si nanorods, which have an average radius smaller than about 27 a_0 as a difference between the first conductive state and the donor ground state. We have found that the binding energy is around 1.5 eV, while the conventional method results an increasing function by reducing the nanorod's radius. The difference is due to the fact that the conventional method does not include the hybridization between the P electron states and Si electron states at the first conductive state. As the size decreases below 27 a_0, the first conductive states are capped near the tops of the atomistic effective potentials at the P donor sites. This causes the binding energy in small nanorods, which are smaller than 27 a_0, to weakly depend on the size when the size continues to decrease. This fact signifies a good tolerance of the binding energy, which governs the operating temperature of the single dopant-based transistors in practice. The transmission spectra, which reflect into the transport properties of electrons in SNRDs, show consistent results with the PDOS-3DWFs method and this fact proves the validity of our new method.

ACKNOWLEDGMENTS

The research was partially supported by the Grants-in-Aid for Scientific Research from the Ministry of Education, Culture, Sports, Science, and Technology in Japan (KAKENHI No. 23226009).

[1]P. M. Koenraad and M. E. Flatt, Nature Mater. **10**, 91–100 (2011).
[2]M. Fuechsle *et al.*, Nature Nanotechnol. **7**, 242–246 (2012).
[3]G. P. Lansbergen *et al.*, Nature Phys. **4**, 656–661 (2008).
[4]S. Markov, B. Cheng, and A. Asenov, IEEE Electron Device Lett. **3**(3), 315–317 (2012).
[5]P. Andrei and I. Mayergoyz, Solid-State Electron. **47**, 2055–2061 (2003).
[6]T. Ohtou, N. Sugii, and T. Hiramoto, IEEE Electron Device Lett. **28**(3), 740–742 (2007).
[7]Y. Yasuda, M. Takamiya, and T. Hiramoto, IEEE Trans. Electron Devices **47**(10), 1838–1842 (2000).
[8]A. Asenov, IEEE Trans. Electron Devices **45**(12), 2505–2513 (1998).
[9]A. Asenov and S. Saini, IEEE Trans. Electron Devices **46**(8), 1718–1724 (1999).
[10]H. Sellier *et al.*, Phys. Rev. Lett. **97**, 206805 (2006).
[11]D. Moraru *et al.*, Nanoscale Res. Lett. **6**, 479 (2011).
[12]E. Hamid *et al.*, Phys. Rev. B **87**, 085420 (2013).
[13]Y. M. Niquet, C. Delerue, G. Allan, and M. Lannoo, Phys. Rev. B **62**(8), 5109 (2000).
[14]D. V. Melnikov and J. R. Chelikowsky, Phys. Rev. Lett. **92**(4), 046802 (2004).
[15]M. Diarra, Y. Niquet, C. Delerue, and G. Allan, Phys. Rev. B **75**, 045301 (2007).
[16]R. Rurali, B. Aradi, T. Frauenheim, and A. Gali, Phys. Rev. B **79**, 115303 (2009).
[17]G. Cantele *et al.*, Phys. Rev. B **72**, 113303 (2005).
[18]C. R. Leao, A. Fazzio, and A. J. R. Da Silva, Nano Lett. **8**(7), 1866–1871 (2008).
[19]T. L. Chan, M. L. Tiago, E. Kaxiras, and J. R. Chelikowsky, Nano Lett. **8**(2), 596–600 (2008).
[20]Z. Zhou, M. L. Steigerwald, R. A. Friesner, and L. Brus, Phys. Rev. B **71**, 245308 (2005).
[21]D. V. Melnikov and J. R. Chelikowsky, Phys. Rev. B **69**, 113305 (2004).
[22]See http://www.openmx-square.org/ for more detail of the computational software used in this research.

[This article is copyrighted as indicated in the article. Reuse of AIP content is subject to the terms at: http://scitation.aip.org/termsconditions. Downloaded to] IP: 150.65.166.110 On: Tue, 21 Oct 2014 01:57:17

[23]P. Hohenberg and W. Kohn, Phys. Rev. **136**, B864 (1964); W. Kohn and L. J. Sham, *ibid.* **140**, A1133 (1965).
[24]G. B. Bachelet, D. R. Hamann, and M. Schluter, Phys. Rev. B **26**, 4199 (1982).
[25]N. Troullier and J. L. Martine, Phys. Rev. B **43**, 1993 (1991).
[26]L. Kleinman and D. M. Bylander, Phys. Rev. Lett. **48**, 1425 (1982).
[27]P. E. Blochl, Phys. Rev. B **41**, 5414 (1990).
[28]I. Morrison, D. M. Bylander, and L. Kleinman, Phys. Rev. B **47**, 6728 (1993).
[29]T. Ozaki and H. Kino, Phys. Rev. B **69**, 195113 (2004).
[30]J. P. Perdew, K. Burke, and M. Ernzerhof, Phys. Rev. Lett. **77**, 3865 (1996).
[31]T. Ozaki, K. Nishio, and H. Kino, Phys. Rev. **81**, 035116 (2010).
[32]V. A. Belyakov and V. A. Burdov, Phys. Lett. A **367**, 128–134 (2007).
[33]T. Ozaki and H. Kino, Phys. Rev. B **72**, 045121 (2005).
[34]P. Parida, E. A. Basheera, and S. K. Pati, J. Mater. Chem. **22**, 14916–14924 (2012).

[This article is copyrighted as indicated in the article. Reuse of AIP content is subject to the terms at: http://scitation.aip.org/termsconditions. Downloaded to] IP: 150.65.166.110 On: Tue, 21 Oct 2014 01:57:17